

OCEANOGRAPHIC RESEARCH AT APL

F. S. Billig
C. J. Gundersdorf
L. J. Crawford

An extended series of detailed oceanographic measurements was conducted near St. Croix, U.S. Virgin Islands, from October 1974 through August 1976, using the APL fleet of research vessels. A description of the instruments, a sampling of the measurements, and a discussion of the ocean's physical features in the lee of St. Croix are presented.

Introduction

From its very modest beginning in 1964, the "fleet" of research vessels (R/V's) of the Applied Physics Laboratory of The Johns Hopkins University (APL/JHU) now contributes significantly to the rapidly growing data base of oceanography. The strong inflationary pressures that began to build during the Vietnam conflict, coupled with the intense competition for the dwindling resource of Navy ships, prompted the development of an alternate source of vessels that could be used to assist the U.S. Navy in important sea testing programs. Consequently, the first APL/JHU R/V, the *Sinbad*, was leased in 1964 to conduct acoustical/sonar test operations off the coast of Florida.

As shown in Table 1, of the thirteen vessels that have belonged to the APL/JHU fleet, five are currently in service. Two of these, the R/V *Cove* and the R/V *Cape*, were formerly U.S. Navy wooden-hulled inshore minesweepers that were provided to APL/JHU in 1970 and 1974 and have served as "flagships" of the research fleet since being converted to highly sophisticated floating laboratories. The remainder of the current fleet, as well as most of their predecessors, have been donated to the University, free of encumbrance, from philanthropic sources. Although all are small by comparison with the research vessels generally used by government maritime agencies and the larger oceanographic institutions, their very low operating cost

and extremely versatile navigational capability make them valuable for the Navy. Generally, operations are arranged to permit supply from shore bases at no greater than two- to three-week intervals. Frequently, exercises involve operations of several of the R/V's coordinated with larger R/V's, Navy surface vessels, submarines, and aircraft.

All the vessels are equipped with modern navigational aids, including the latest satellite receivers, so that the precise location and movement of the test vehicles are known at all times. On-board communication systems provide a direct link to APL/JHU in Howard County, Maryland, and the progress of the experiments can be closely monitored on shore. The communication systems are complemented by an array of sophisticated scientific instrumentation and recording systems, some of which will be discussed in detail.

Initially, the R/V's were primarily involved in recording and analyzing acoustic data. However, the measurement programs have grown to include detailed mapping of the physical properties of the ocean and of the ocean-atmosphere interface. In August 1973, the R/V *Cove* was used to obtain radiometric clutter measurements with an ultra-sensitive two-wavelength radiometer in waters north of Nassau, in the Bahamas.¹ Other param-

¹ Gasparovic, R. F., Emmons, G. H., and Tubbs, L. D., "Two Wavelength Measurements of the Ocean Surface Radiometric Clutter," *Proc. IRIS 19* (1974).

Table 1
DESCRIPTION OF APL OCEANOGRAPHIC RESEARCH VESSELS

R/V	Type	Acquired		Dimensions (ft)		Max. Draft (ft)	Displacement (tons)	Speed (kt)		Range (nmi)	Accommodations	
		When	How	Length	Max. Beam			Cruise	Max.		Crew	Scientists
<i>Sinbad</i>	Power cruiser	1964	Leased	57.8	14.8	3.9	39	16				
<i>White Cirrus</i>	Ketch motor sailer	1966	Private donation	50.9	14.2	7	35.8	8.5			2	5
<i>Sorrento</i>	Motor sailer	1967	Leased	81.1	19.8	7.0-13.9	49	9	10		4	7
<i>White Cirrus II</i>		1968	Private donation	53.5	13	6.2-10.2		7		300	5	3
<i>Bonnie Dundee</i>	Motor sailer	1969	Private donation	85	18	6	60	9	10	1000	6	4
<i>Cove*</i>	Minesweeper	1970	U.S.N.	111.8	24.5	10	239	9.5	12	1987	8	11
<i>Ultimate</i>	Cruising yacht	1971	Private donation	87	18	5	98	9.5	12	600	2	7
<i>Cape*</i>	Minesweeper	1974	U.S.N.	111.8	24.5	10	239	9.5	12	1987	8	11
<i>Beayondan</i>	Aluminum motor sailer	1975	Private donation	83	18	6	56	9	10	900	5	4
<i>Stranger</i>	Aluminum motor sailer	1975	Private donation	62	21	4	26	7	8	1000	2	8
<i>Southern Star*</i>	Aluminum power-sloop	1975	Private donation	75.3	18	7.5-14.1	65	8.3	10.5	1300	5	5
<i>Constance*</i>	Cruising yacht	1977	Private donation	83	19.9	5	108	12.5	15.5	480	4	6
<i>Island Waters*</i>	Cruising yacht	1977	Private donation	82	20	9.9	117	11	12	5000	4	2

*In service.

eters measured included the height of surface waves, subsurface water temperature and salinity, humidity, sky radiance (in the 8 to 13 μ m region), and wind speed and direction. In the fall of 1973, R/V *Cove* participated in IWEX (Internal Wave Experiment), a joint exercise with the Woods Hole Oceanographic Institution (WHOI). WHOI deployed a 6000-m-long deep-sea trimooring in the Sargasso Sea to measure the vector wave number and frequency spectrum of motions in the main thermocline over a range of space and time scales appropriate to internal gravity waves.² R/V *Cove* made measurements with a towed thermistor chain and took conductivity and temperature surveys in the general vicinity of the mooring.

During the period October 1974 through August 1976, R/V's *Cape*, *Cove*, *Beayondan*, *Stranger*, and *Southern Star* participated in an extended series of detailed measurements near the island of St. Croix, using sophisticated instrumentation systems. This article discusses the instru-

mentation systems, a sampling of the measurements made with each system, and new ways to process and display the data. It also describes some of the physical features of the ocean in the lee of St. Croix.

All the tests described were made on the St. Croix Underwater Tracking Range (UTR) located on the west coast of the island, which was chosen for several reasons. First and foremost was the accurate three-dimensional tracking capability for simultaneously tracking and controlling several systems. Second, one of the objectives of the test series was to develop systems and techniques that could readily be adapted for open ocean testing; many features of the water structure in the area were known to be typical of the open ocean environment. Third, operations on the island's protected leeward side permitted the deployment and operation of the sophisticated equipment in a relatively calm environment. Fourth, since the St. Croix range is used extensively in developing and testing many systems, it is important to improve the definition of the physical properties of the ocean's upper 300 m in this region. Intrinsic to the design of the systems used in the test operations

² Briscoe, M. G., "Preliminary Results from the Trimooored Internal Wave Experiments (IWEX)," *J. Geophys. Res.* **80**, 3872-3884 (1975).

were the scales of the physical features to be resolved. Typically, length scales from several centimeters to a few kilometers and time scales from minutes to two months were involved.

Descriptions of Instrument Systems

SPURV System

The Applied Physics Laboratory of the University of Washington (APL/UW) has developed a series of self-propelled underwater research vehicles (SPURV's) as instrumentation platforms for conducting oceanographic research. (Reference 3 describes SPURV's in detail.) *SPURV II*, one of the remotely controlled free-swimming vehicles (Fig. 1), was modified in accordance with specifications provided by APL/JHU for the St. Croix experiments. The main body of the vehicle is 9.8 ft long and consists of a central cylinder, 20-in. OD, and two spheric-ogive end sections. The vehicle can be located during recovery operations by means of the radio beacon antenna, which has a flashing light module at the tip and is mounted on a very flexible spring so that it will trail close to the hull when the vehicle is submerged. The 75-kHz acoustical pinger for range tracking is located on the ventral surface. Propulsion is provided by a 2400-rpm, 1-hp permanent magnet motor that drives a 14-in.-diameter three-bladed propeller. The power source consists of two banks of 16 silver-zinc batteries connected in parallel to form a 36-V, 340-Ah power supply. A second set of batteries provides a 24-V, 65-Ah source that powers the instrumentation and control surfaces.

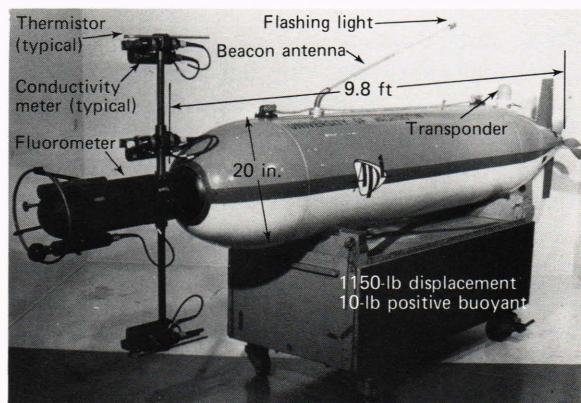


Fig. 1—*SPURV II*.

³ Widditsch, H. R., *SPURV—The First Decade*, APL/UW Report 7215 (1973).

A Vibratron pressure transducer is located near the tail section; other sensor instrumentation is located on 3.23-ft vertical strut attached to the nose. Mounted on the strut and support system are three temperature sensors, three conductivity sensors, and a fluorometer. The characteristics of the sensors are listed in Table 2. Sampling rates are typically either 5 or 10 per second, and time constants for all sensors are 50 ms.

Table 2

CHARACTERISTICS OF SPURV II INSTRUMENTATION

Measurement	Resolution	Accuracy
Temperature (°C)	0.005	0.01
Conductivity (μmho/cm)	0.6	10
Dye (g/cm ³)	10 ⁻¹²	0.1% full scale
Pressure (depth) (m)	0.03	0.1

The dynamic range of the rhodamine dye-sensing fluorometer is about a factor of 10³; it can be preset for any desired range of concentrations between 10⁻⁶ and 10⁻¹² g/cm³. Data from all sensors are recorded on a 7-in. reel of half-inch nine-track magnetic tape at a nominal rate of 10 samples per second per channel. Control-surface deflections, vehicle attitude, and other vehicle-related functions are also recorded on the tape for off-line analysis. The tape can accommodate about 6 h of recording; this closely matches the 7-h life of the propulsion power system before recharging is required.

Communication with *SPURV II* is provided by an array of transponders, located on the hull of a support ship, that can operate at slant-range distances up to 2000 m. Transmission to the vehicle is at 20 and 22 kHz; the vehicle replies at 26 and 28.9 kHz. On board the surface vessel is a PDP-11 computer system that is used for processing and displaying tracking and dye-sensor information in real time and for providing the maneuver-command logic.

SPURV II is a good platform for making oceanographic measurements because it can be accurately controlled from its support ship. Prior to launch, the vehicle and the support ship are oriented in a prescribed direction and the yaw control system is nulled. Thereafter, azimuthal reference of *SPURV II* is maintained by a self-leveling gyro. Errors in heading angle during one duty cycle are held to less than 2°. Following launch, the vehicle swims in accordance with commands from the support ship. Programs have been developed for the

PDP-11 computer that allow the vehicle to follow prescribed courses while either maintaining constant depth or performing complex maneuvers in both the vertical and horizontal planes.

T-F Chain

The thermistor-fluorometer (T-F) chain is a 750-ft cable with a plastic nose and with tail fairings to reduce drag. These fairings, which house the thermistors and their associated electronics and electrical connectors, are streamlined to reduce drag. Each fairing is 4 in. in length and is attached to adjacent fairings in such a way that it is only partially constrained in the transverse direction. Thus, the cable is free to twist and thereby remains aligned to the local flow direction, which typically varies considerably along the length of the cable. Figure 2 shows the chain deployed from the R/V *Cape*. As currently configured, it can be towed at speeds of 4 to 8 kt without excessive "kiting" (lateral displacement). It was designed and built at APL/JHU with major subcontractual support from Sippican Corp. and Fathom Oceanology, Ltd. (Reference 4 describes the system com-



Fig. 2—R/V *Cape* towing T-F chain.

⁴ Mobley, F. F., Sadilek, A. C., Gundersdorf, C. J., and Speranza, D., "A New Thermistor Chain for Underwater Temperature Measurement," *Oceans '76 Conference Record* (IEEE Publication No. 76) (1976).

pletely.) As used in this measurements program, the instrumentation complement included 42 thermistors, 15 fluorometers, six depth transducers, and several acoustical navigation aids. The analog signal from the 63 sensors was sequentially digitized 20 times per second with 12-bit resolution, and was then recorded on digital tape.

Figure 3 schematically illustrates the chain and shows some of its components. In a typical test, the chain is towed across a dye track that was laid earlier, and measurements of dye concentration, temperature, and pressure are made. Thermistors, spaced every 6.5 to 13 ft along 460 ft of the cable, were designed to obtain temperature measurements with a relative accuracy of $\pm 0.01^{\circ}\text{C}$ rms and a resolution of $\pm 0.001^{\circ}\text{C}$ rms in the range of 20 to 30°C with a response-time constant ($1/e$) of 180 ms. (Subsequent improvements in the design have demonstrated time constants of 50 ms.) The fluorometers are 6.4-in.-diameter streamlined bodies that are attached to the chain by mechanical and electrical quick-connects during deployment. Water flowing through the devices is illuminated by an incandescent lamp that is filtered to a bandwidth from 494 to 547 nm, causing fluorescence of rhodamine dye previously dispensed in the water. Emitted light from the fluorescing dye passes through a filter set and is detected by a silicone photodiode. Dye concentrations of 1 part in 10^{11} can be measured with an accuracy of 5% over the entire scale and with a time constant of 0.5 s.

The Sensatec 0- to 300-psi depth-sensing pressure transducers are specially calibrated at APL/JHU. A 4.5-ft-long towed body, loaded with lead to give it an in-water weight of 750 lb, is attached to the end of the chain. Within the body are an acoustic range-pinger to provide tracking signals, a pressure transducer to measure the depth, and a broadband acoustic-noise generator for active ranging.

CTD Systems

Two conductivity-temperature-depth (CTD) microprofiler systems were used in these tests: a Plessey CTDSV (SV refers to a sound-velocity sensor, which is included in this profiler) and a Neil Brown CTD. Figure 4a is a schematic illustration of the Plessey unit. The platinum-resistance thermometer, conductivity, depth/pressure, and sound-velocity sensors located in the bottom of the

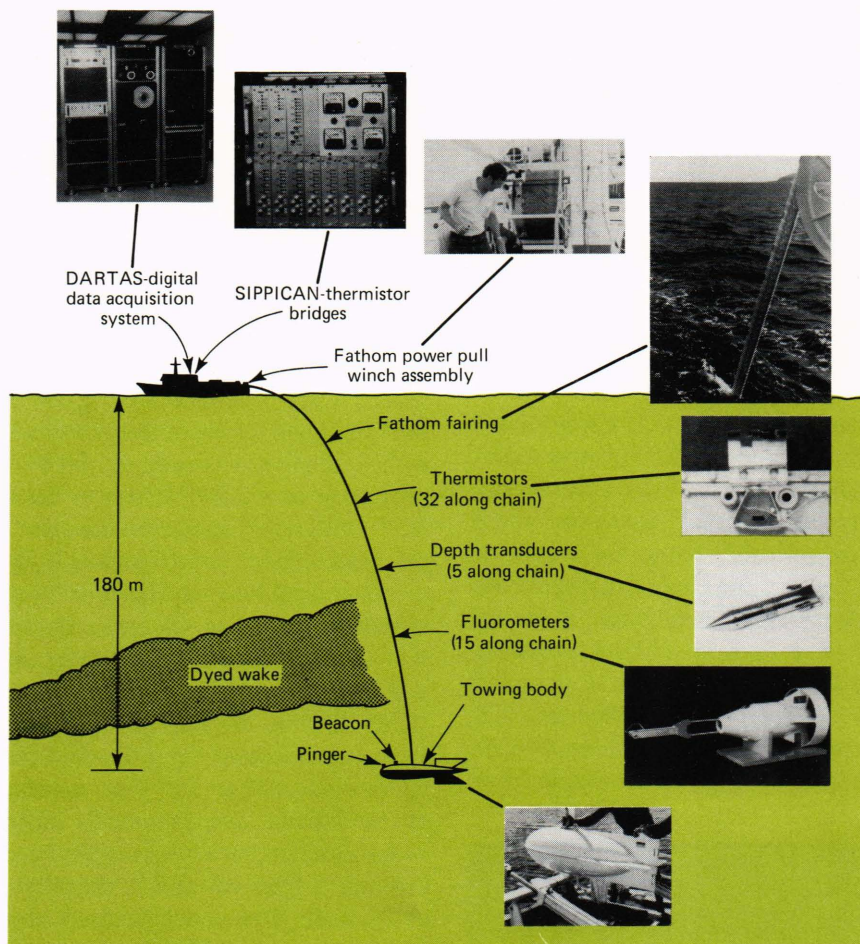


Fig. 3—T-F chain.

device are protected by a guard ring. The system electronics are housed in the unit's main cylinder. Included therein are an AC voltage-to-frequency converter and a mixer that receives and regulates power from the deck and transmits it to the sensors. The converter also multiplexes and amplifies the FM signals and transmits them up the sea cable.

Figure 4b shows the Neil Brown microprofiler; it can be used even at the microstructure scale of temperature and conductivity profiles. Conductivity is measured by a miniature (8-mm-long, 2-mm-ID) four-electrode cell. Temperature is sensed by a combination of a fast thermistor and a platinum-resistance thermometer. The main body of the instrument, which is 30 in. long and 8 in. OD, houses the electronics. Signals from the conductivity, temperature, and pressure units are digitized and transmitted to the terminal equipment on the deck along a single-conductor shielded

cable. Each instrument is sampled 30 times per second. Specifications for the two CTD systems are given in Table 3.

As supplied by the manufacturer, the Plessey CTD has an effective time constant for temperature measurements of 0.35 s. However, a way to process the data⁵ using a correction obtained from the sound velocity measurement has reduced the constant to 0.10 s. In most range operations, sound velocities are deduced from temperature measurements made with expendable bathothermographs (XBT's) at infrequent intervals. With the Plessey system, the velocities are measured directly to provide frequent updating to the range calibration system, thus significantly improving the tracking accuracy.

⁵ Mack, S. A., Wenstrand, D. C., and Coates, G. M., "Horizontal and Temporal Variability of the Brunt-Väisälä Frequency Off the West Coast of St. Croix," *EUS Trans.* 46, 1005 (1975).

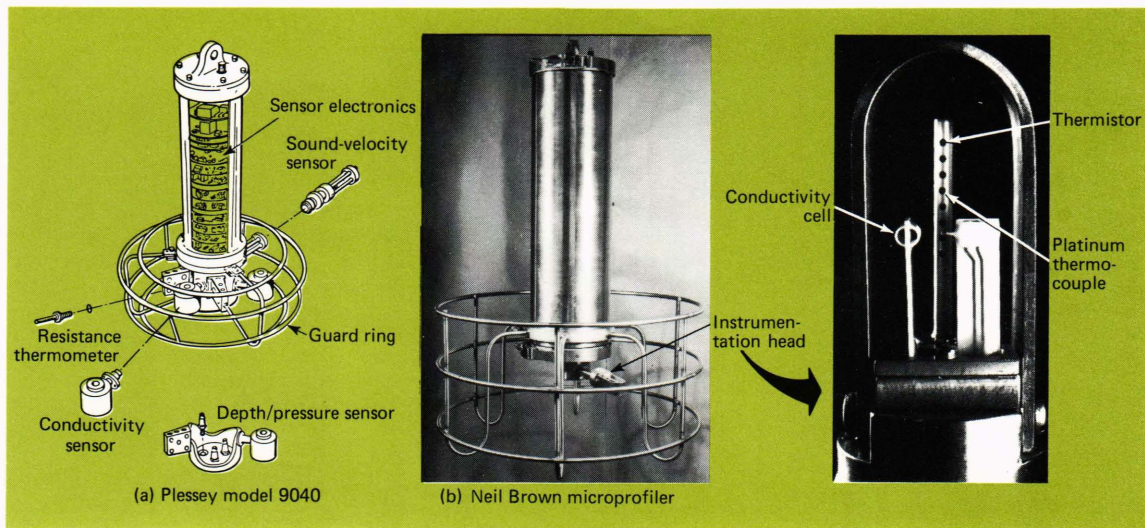


Fig. 4—CTD systems.
 (a) Plessey model 9040.
 (b) Neil Brown microprofiler.

Table 3
 MANUFACTURER'S SPECIFICATIONS OF PLESSEY MODEL 9040 CTDSV

Parameter	Time Constant (s)	Range	Resolution (Digital Data Logger)	Accuracy	Repeatability
Temperature (°C)	0.35	-2-35	±0.001	±0.02	±0.01
Conductivity (mmho/cm)	0.1	10-60	±0.002	±0.03	±0.02
Depth (m)	0.1	0-1800	±0.11	±4.5	±1.8
Sound Velocity (m/s)	0.1	1400-1600	±0.006	±0.3	±0.1

MANUFACTURER'S SPECIFICATIONS OF NEIL BROWN CTD

Parameter	Time Constant (ms)	Range	Resolution	Stability	
				Short Term (3 months)	Long Term (6 months)
Temperature (°C)	30	0-±35	±0.0005	±0.003	±0.005
Conductivity (mmho/cm)	30	20-65	±0.001	±0.003	±0.005
Depth (m)	100	0-1500	±0.0015% of full scale	±0.075% of full scale	±0.1% of full scale

The shipboard equipment records the signals on strip charts, on nine-track digital magnetic tape, and on a Hewlett-Packard printer that can be set to print out one complete set of data each second in engineering units. The magnetic tape unit can accept four complete sets of data per second.

Current-Shear Profiler

The current-shear profiler, a device built by APL/JHU, is used in conjunction with an acoustic range to measure the vertical profile of both horizontal components of ocean current. The acoustic range tracks the profiler as it slowly sinks and re-

records the measured coordinates on magnetic tape. From this position-time series, the profiler's rate and direction of horizontal movement at each depth can be computed, thereby giving the water velocity.

Figure 5 is a photograph of the profiler taken just before deployment from the R/V *Cape*. It consists of a 5-ft-long, 12-in.-diameter pressure vessel that houses a crystal clock and other electronics used to generate a precisely timed 75-kHz acoustic pulse. The times of arrival of a given acoustic pulse at each of four bottom-mounted hydrophones and the known time when the pulse was emitted are used to compute the time of flight to each hydro-

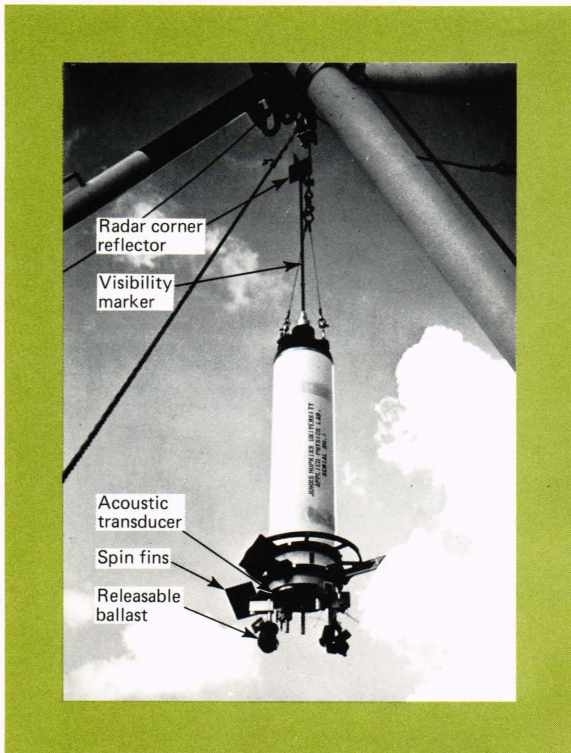


Fig. 5—Ocean current-shear profiler.

phone. From a knowledge of the relative positions of the hydrophones, the position of the profiler relative to the center of the array can be computed.

While the absolute accuracy of this position determination relative to local geography is ± 25 ft, repeatability and resolution are much better, approximately ± 1 ft each. By averaging over 60 s of data (47 data points), the positional error can be reduced to ± 0.15 ft, giving a random error in velocity of less than 1 mm/s. The profiler's crystal clock drifts at a rate of less than $10 \mu\text{s}$ in 1 min, giving rise to a systematic error in position that builds at a rate of somewhat less than 0.05 ft/min. This causes a systematic error in velocity of 0.3 mm/s.

Current-Meter Mooring

The current-meter mooring shown in Fig. 6 was deployed in 972 m of water on February 20, 1976, by WHOI.⁶ The $\frac{3}{16}$ -in.-diameter torque-balanced wire rope was anchored by five railroad

⁶ Tarbell, S., Payne, R., and Walden R., *A Compilation of Moored Current Meter Data and Associated Mooring Action Data From Mooring 592: Vol. XIV (1976 Data)*, Woods Hole Oceanographic Institute Report 77-41 (1977).

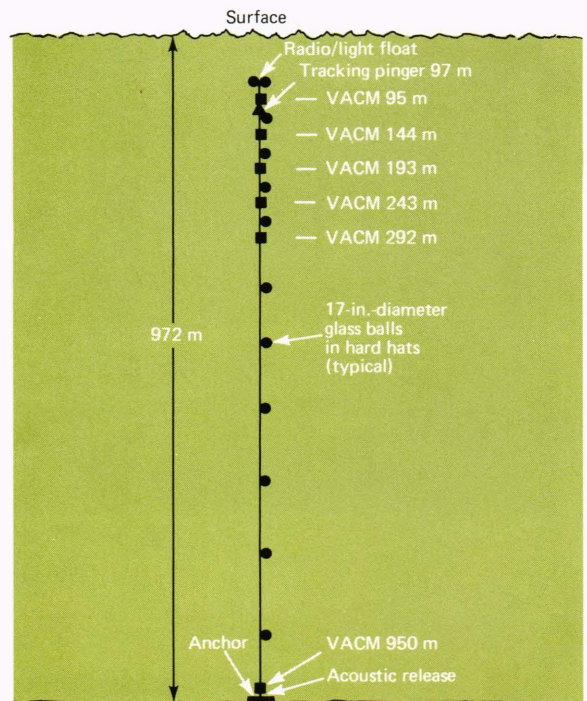


Fig. 6—Schematic illustration of Woods Hole current-meter mooring.

wheels having a net weight in water of 3000 lb. On April 27, 1976, the system was recovered when the anchor was released by actuating an acoustic release. A radio/light combination was attached to the near-surface end of the wire at a nominal depth of 65 m to help locate the system during recovery operations. Flotation throughout the length of the mooring was provided by 17-in.-diameter glass spheres, housed in "hard hats" as shown in Fig. 6. An acoustic tracking pinger was attached to the wire 97 m below the surface as a means of providing a position/time series for determining the motion of the mooring. This unit radiated acoustic pulses at 75 kHz for the first three days after deployment before its battery power was exhausted.

The remaining instrumentation consisted of six vector-averaging current meters (VACM's) that measure and record a component of the water velocity, the current's direction relative to the unit, the unit's magnetic orientation, and the local temperature. Four of the five upper units located at depths of 95, 144, 193, and 243 m operated satisfactorily, recording averaged data once every 56.25 s. The fifth unit, located at 292 m, failed to operate. The sixth unit, located just above the ocean floor at 950 m, recorded averaged data every 112.5 s for 64 days. However, its rotor pivot bearing

was broken during launch so that only average temperature was recorded.

These units can measure currents over the range of 2.5 to 300 cm/s and can resolve compass and vane direction to 2.8° . The operating temperature range is -2 to $+35^\circ\text{C}$ with a thermistor accuracy of $\pm 0.10^\circ\text{C}$.

Dye-Dispensing System

The details of the dispensing system used to lay down dye trails for chain-crossing runs are shown in Figs. 7a and 7b. Rhodamine dye, stored in a reservoir, was pumped through a filter and flowmeter into a $\frac{1}{4}$ -in.-diameter hose that is part of a cable ensemble deployed from a winch. The hose terminates in the hub of the injector ring shown in detail in Fig. 7b. Each radial support arm and the outer hexagonal ring contain 0.020-in.-diameter holes that are spaced 3 in. apart on alternate sides of the members. The members are made of aluminum tubing that has a $1\frac{1}{2}$ -in. OD and is 0.125 in. thick. The tubing has a $\frac{1}{16}$ -in.-thick aluminum tail fairing to reduce drag.

The tow cable terminates 7 ft below the dye-ring tow point. A hydrodynamic depressor is attached to the end of the tow cable to help keep the ring at the prescribed depth. Mounted on the depressor are a pressure transducer and two acoustic pingers. Depth is obtained from the pressure measurement; the pingers provide acoustic pulses for tracking

and ranging. The time-code pulses from the 45-kHz pinger were used for establishing range to SPURV II in other runs. The 75-kHz pinger is used by the UTR for tracking the coordinates of the depressor.

Test Operations

Figure 8, a schematic illustration of the St. Croix UTR, shows the location of the oceanic-background measurements relative to the range-tracking arrays. At the time of the tests, the range comprised 11 three-dimensional tracking arrays (increased to 13 in the spring of 1977) that provided coverage of approximately 6 square miles of surface. Each array (represented schematically in Fig. 8 by a dashed circle) is located about 1000 m deep on the ocean floor and is equipped with five hydrophones and a level-sensing system that indicates array tilt. Acoustic pulses from all test-platform pinger packages located on the range are converted to electrical pulses by the array hydrophones and transmitted with tilt information by cable to the Sprat shore installation. The pulses are time-tagged and processed by logic receivers that generate time values in digital form and send them to a computer. The computer uses the digitized information to compute the range position of the test-platform and to store the data on magnetic tape. Corrections for variations in sound velocity

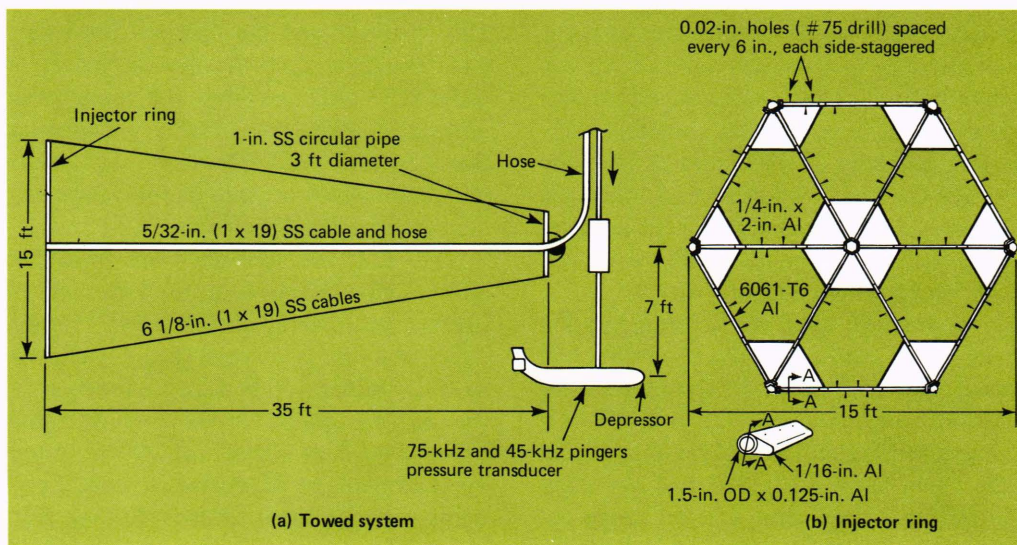


Fig. 7—Dye-dispensing system.
(a) Towed system.
(b) Injector ring.

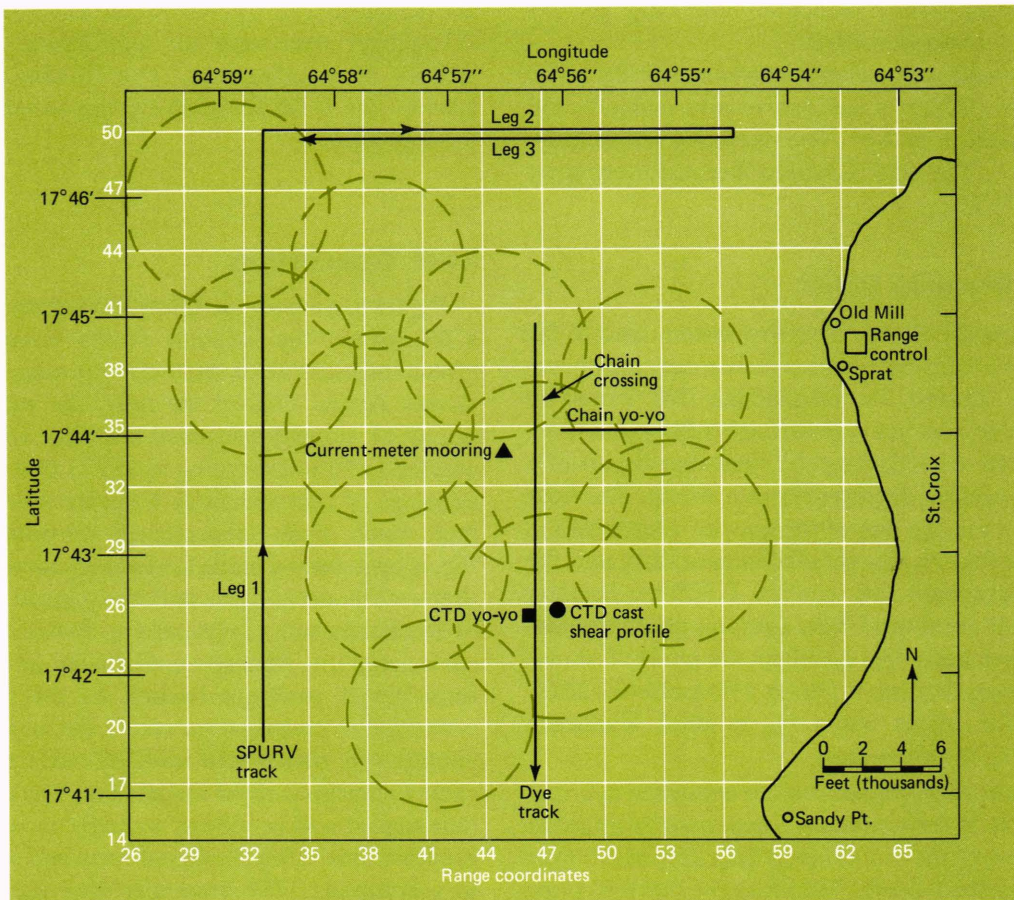


Fig. 8—Schematic illustration of the St. Croix UTR showing locations of background measurements.

with depth, for array tilt, and for minor time delays are included in the position computations. Data transformed from array coordinates to range coordinates are displayed in real time on an x-y plotter, a digital display panel, and a digital printer. Up to four objects can be tracked simultaneously with a relative accuracy of ± 1 ft and an absolute accuracy of 25 ft. The position of each object is determined every 1.31 s from the acoustical pulses that are generated with a pulse width of 1.2 ms and a carrier frequency of 75 kHz.

The run geometries and the instrumentation platform positions (shown in Fig. 8), although representative, are only a small sample of the complete operations. The data selected from SPURV are from the second leg of a three-leg run made on January 22, 1976. On this leg, SPURV was commanded to follow a track due east on range coordinate N50 at a depth of 135 m. The T-F chain-crossing run was made on January 26. Dye was dispensed from a 15-ft hexagonal injector that was

towed from the R/V *Cove* on a track due south on E46.3. The dye injector crossed N37.3 at 13h:57m:44s and the chain crossed the track at 14h:06m:27s; thus the measurements are for a wake 523 s old. The other T-F chain data are from August 23, 1976, when the R/V *Cape* was heading due west on N34.9. The chain was deployed to a maximum depth of 96 m and it "yo-yoed" through a layer 10 m deep for 10 min.

The CTD measurements are from February 9 and August 21, 1976. In the latter run, the CTD profiler was lowered at N25.6 E45.8 to a maximum depth of 44 m. It yo-yoed through a depth of 18 m at 20-s intervals for 39 min. On the February 9 run, the hydrographic variables were measured at N25.8 E47.4 to a depth of 300 m. Simultaneous measurements of the current's vertical profile were made with the shear profiler. Finally, during February 20 to April 27, 1976, measurements by the moored current meter were made at depths from 95 to 950 m at N33.65 E45.0.

Discussion of Measurements

The data obtained from the SPURV II run geometry shown in Fig. 8 were analyzed by APL/UW.⁷ They are summarized in Fig. 9, which shows

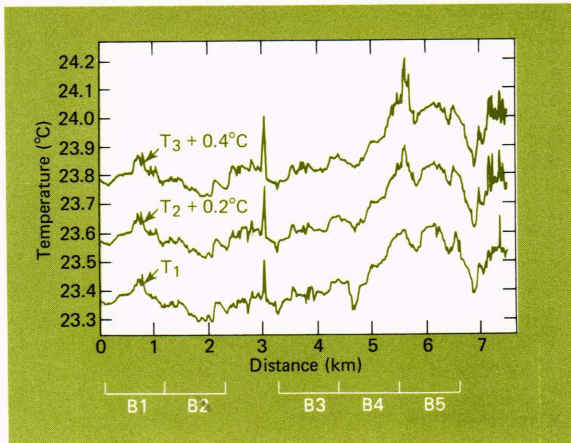


Fig. 9—Temperature traces from leg 2 of the SPURV run on January 22, 1976.

the temperature traces obtained from the three thermistors during the second leg at a constant depth of 135 m. The corresponding depths of the transducers were 135.52, 134.80, and 134.46 m, respectively, for traces T1, T2, and T3. The temperature on the ordinate for T2 and T3 has the same scale factor as T1 but is offset 0.2°C for T2 and 0.4°C for T3, for clarity. For purposes of analysis, five sets of 4096 typical data points each, labeled B1 through B5 in Fig. 9, were examined for each sensor. The region between B2 and B3 was not included because the vehicle had inadvertently undergone a depth change. For each data set listed in Table 4, the variance V , in temperature was computed, where

$$V = \frac{1}{n} \sum_{i=1}^n (t_i - \bar{t})^2, \text{ and} \quad (1)$$

$$\bar{t} = \frac{1}{n} \sum_{i=1}^n t_i. \quad (2)$$

(t_i is the temperatures at the n points in each set—in this case 4096—and t is the arithmetic mean temperature.) From Table 4 it can be seen that, with the exception of thermistor T3 during time interval B5, the variances in the measurements made by the three thermistors are nearly the same

in each time segment. Moreover, V has about the same value for all segments other than B4.

The causes of the observed temperature fluctuations are of considerable interest in understanding ocean dynamics in the lee of an island. Possible sources include internal waves, water-mass inhomogeneities, eddies shed from the island, or other disturbances generated by flow around St. Croix. Some insight as to whether internal waves could be the source can be gained by comparing the spectrum of the measurements with that postulated by Garrett and Munk (GM 75) for the open ocean.⁸

Table 4

VARIANCE IN TEMPERATURE ($\times 10^3$ °C²) FOR SELECTED DATA SETS FROM SPURV TESTS

Sensor	B1	B2	B3	B4	B5	Average
T1	0.709	0.535	0.522	4.78	0.879	1.50
T2	0.777	0.459	0.519	3.80	0.896	1.29
T3	0.808	0.435	0.586	4.88	0.224	1.39

The GM 75 towed temperature spectrum (TTS) is obtained by multiplying the GM 75 towed displacement spectrum (TDS) by the square of the average vertical temperature gradient, which was 0.04°C/m for the region and time of the SPURV measurements. Reference 9 gives

$$\text{TDS} = \left(\frac{2}{\pi}\right)^3 \frac{f}{N} \left(\ln \frac{N}{f} - \frac{N^2 - f^2}{2N^2} \right) (rt)k^{-2}. \quad (3)$$

Here, f is the local value of inertial frequency. (If a large slab of water is set in motion in the horizontal plane, it will be accelerated at right angles to its velocity vector by the Coriolis force. This slab of water will move in a circular orbit with a period, T , given by

$$T = \frac{1}{f} = \frac{12 \text{ hours}}{\sin \phi},$$

where ϕ is latitude. Moreover, the Coriolis frequency, f , is also the low-frequency cutoff for internal waves.) The horizontal wave number is k and

$$N = \frac{1}{2\pi} \left(-\frac{g}{\rho} \frac{d\rho}{dz} - \frac{g^2}{a^2} \right)^{1/2} \quad (4)$$

is the Brunt-Väisälä (B-V) frequency, which is a

⁷ Ewart, T. E., *Observations from Straightline Isobaric Runs of SPURV*, Preliminary Report for the IAPSO/IAMAP PSII Poster Session of the JOA in Edinburgh (1976).

⁸ Garrett, C., and Munk, W., "Space-Time Scales of Internal Waves: A Progress Report," *J. Geophys. Res.* **80**, 291-297 (1975).

⁹ Desaubies, Y. J. F., "Analytical Representation of Internal Wave Spectra," *J. Phys. Oceanogr.* **6**, 976-981 (1976).

dynamic property that represents the natural frequency of oscillation of a fluid element disturbed from its equilibrium position in a stratified fluid having a density gradient with depth $d\rho/dz$. Here, g is the gravitational constant and a is the speed of sound in water. The remaining terms in Eq. 3, r and t , are empirical constants in the Garrett and Munk model that are adjusted to give the correct spectral level and the observed bandwidth, respectively. For the St. Croix area, $f = 0.025$ cyc/h; measurements from other SPURV runs gave $n = 7.5$ cyc/h, and Ref. 5 suggests a value of 0.1 for rt based on open ocean observations. Using these values yields

$$\text{TTS} = 7.2 \times 10^{-7} k^{-2} \quad (5)$$

Figure 10 compares Eq. 5 with the spectrum obtained from the selected data sets of Fig. 9. The plotted curve was obtained by computing a spectrum, smoothed over equal logarithmic increments in frequency, for each data set and then by averaging all the sets. The close comparison tends to substantiate the contention that some of the physical characteristics of this water mass are similar to the open ocean. Similar results were obtained from analyzing leg 3 (Fig. 8), but leg 1 showed markedly higher fluctuations throughout the spectrum.

Figure 11 is a typical time-series plot of selected thermistor, fluorometer, and pressure data from a run made with the T-F chain. In this run, the chain was towed diagonally across a dye patch that had been laid down with the injection shown in Fig. 7 centered at a depth of 100 m (Fig. 8). Tem-

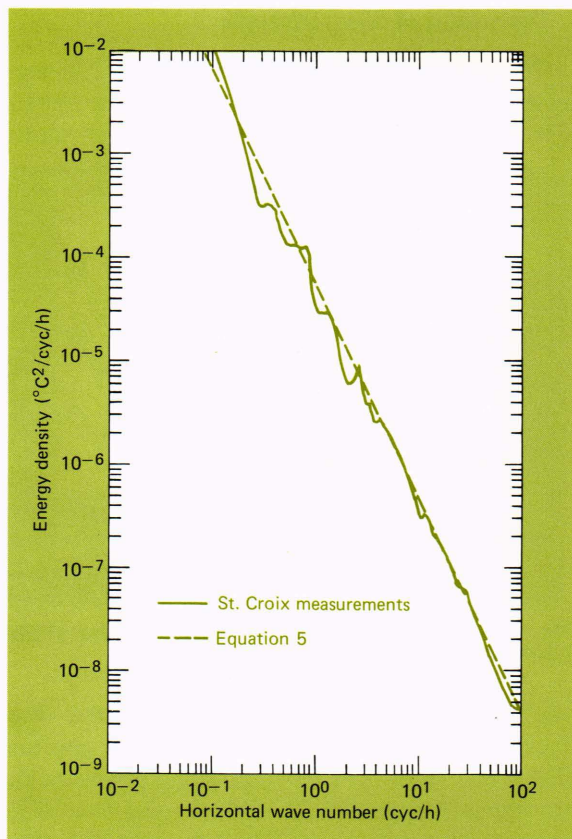


Fig. 10—Towed temperature spectrum from leg 2 of SPURV run on January 22.

peratures and pressures, converted to depth, are plotted about their respective mean values, which are listed on the right. The mean values were obtained from a time segment of 73 s, which cor-

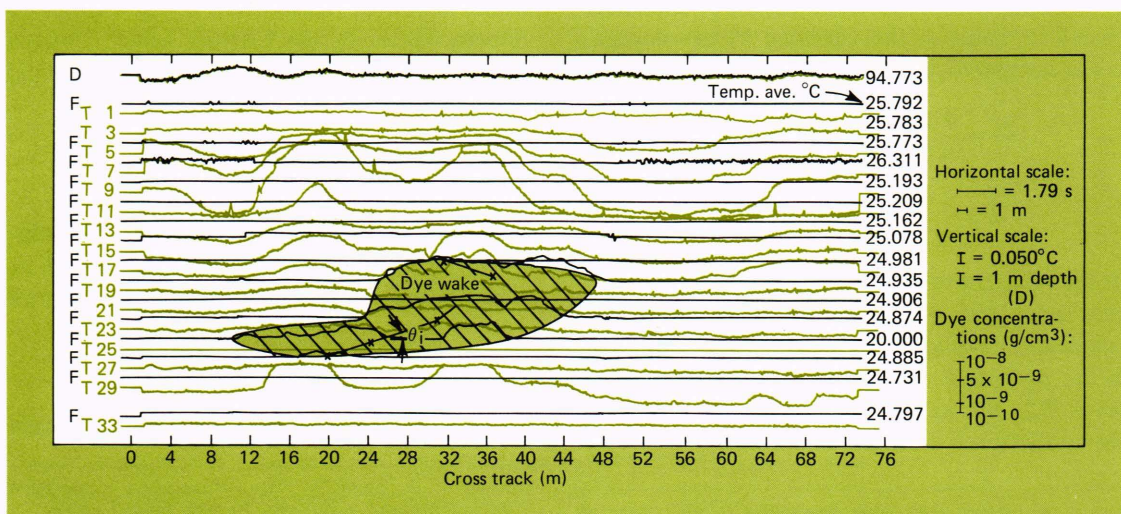


Fig. 11—Dye wake measurements from the T-F chain on January 19.

responds to about twice the interval in which fluorometer readings were above the ambient background level. Dye concentrations are plotted relative to the background level of 0.5×10^{-10} g/cm³. Vertical scale factors for the three types of instruments are shown in the inset. The reference value of the ordinate of each trace is placed at its respective depth. The scale on the abscissa has been adjusted to match that of the ordinate to give a true geometric representation of the dye patch in the cross-track plane (the distance is measured across the dye track, not along the towed-chain track). The dye patch is shown crosshatched where its envelope has been determined by the extent of the perturbations in the outputs of the fluorometers above the background threshold levels.

It is reasonable to assume that the dye patch as initially laid down had the dimensions of the dye injector, which can be approximated as a circle with a diameter of 5 m. From Fig. 11 it can be seen that the dye patch has grown to a height of about 9 m and has a maximum lateral extent of about 36 m. In shear-free stratified flow, Lin et al.¹⁰ show the following correlations for the growth of turbulent wakes laid down by a self-propelled slender body:

$$\frac{H}{D} = (0.43 \pm 0.04) \left(\frac{u}{ND} \right)^{1/4}, \text{ and} \quad (6)$$

$$\frac{W}{D} = 1.1 (Nt)^{1/2} \left(\frac{u}{ND} \right)^{1/4}, \quad (7)$$

where H and W are the mean values of height and width of the wake, D is the initial diameter, t is the age of the wake (523 s in this case), and u is the velocity of the body that created the wake (2.18 m/s in this case). N for this run was 7.5 cyc/h. The resulting values of H and W from Eqs. 6 and 7 were 7.4 to 8.9 m and 21.8 m, respectively.

Thus the calculated height is slightly lower, which may be due to vertical diffusivity that is present in the ocean but not in a towing tank upon which the correlations of Eqs. 6 and 7 were based. Of course, the turbulence levels initially present are also quite different, because not only was the environment different but the "sources" generating the wakes were entirely different.

The lateral distortion of the wake is evidence of

the transverse shear that has been acting on the dye patch since it was laid down 523 s prior to the chain crossing. One way to obtain an equivalent cross section of an unsheared wake is to subdivide the wake cross section into thin horizontal slabs and "restack" all the slabs about a common centerline. When this is done to the wake shown in Fig. 11, the maximum width of the wake is 23 to 25 m. For direct comparison with Eq. 7, 1 to 2 m (equivalent to the integral scale of the turbulence) should be subtracted to obtain a "measured mean" width. Again the agreement of tank and adjusted ocean data is quite good.

The lateral distortion of the cross section can be used to estimate the average cross-track shear by connecting the centers of the elevated portions of the fluorometer traces (the x's in Fig. 11). The shear equals the cotangent of θ (shown in Fig. 11), divided by the age of the wake. For these data the respective shear values for depths of 97.8, 100.8, 103.8, and 105.8 m are -2.3×10^{-3} , 1.4×10^{-3} , 9.1×10^{-3} , and 4.3×10^{-3} per second, respectively.

Among other features that can be identified in Fig. 11 are (a) the relatively greater level of turbulent-like structure in the dye-wake region as shown by the higher incidence of high-frequency fluctuations and (b) the presence of wave-like structure as evidenced by the longer-wavelength perturbations that are coherent over several thermistor traces. One should disregard the coherent "glitches" in the thermistor data (at 20 m cross-track, for example) that result from inadvertent feed-through of the acoustic pinger in the towed body.

Figure 12 shows a time series from a towed yo-yo of the chain. Data from the 35 thermistors and the depth transducer D1 are plotted about their respective mean values. The traces are oriented on the abscissa by locating the mean value at the respective mean depths. (Thermistors T-37, T-22, T-16, and T-9 were inoperative in this run.)

Several interesting features are readily identifiable in Fig. 12. The control of the chain yo-yo is good, as shown by the symmetric sawtooth traces in the D1 output that have an amplitude of 10 m and a period of 49 s. The mixed layer extends to a depth of about 21 m (T-36 passed into the steep-gradient zone only twice at the lower extent of its travel). This is confirmed in the traces of T-35 and T-21 by the flat regions in the portion corresponding to the shallower part of the yo-yo cycle. Be-

¹⁰ Lin, J. T., Veenhuizen, S. D., and Ko, D. R. S., *The Effect of Internal Froude Number on the Stratified Wake of a Self-Propelled Slender Body*, Report 46, Flow Research, Inc., Kent, Washington (1976).

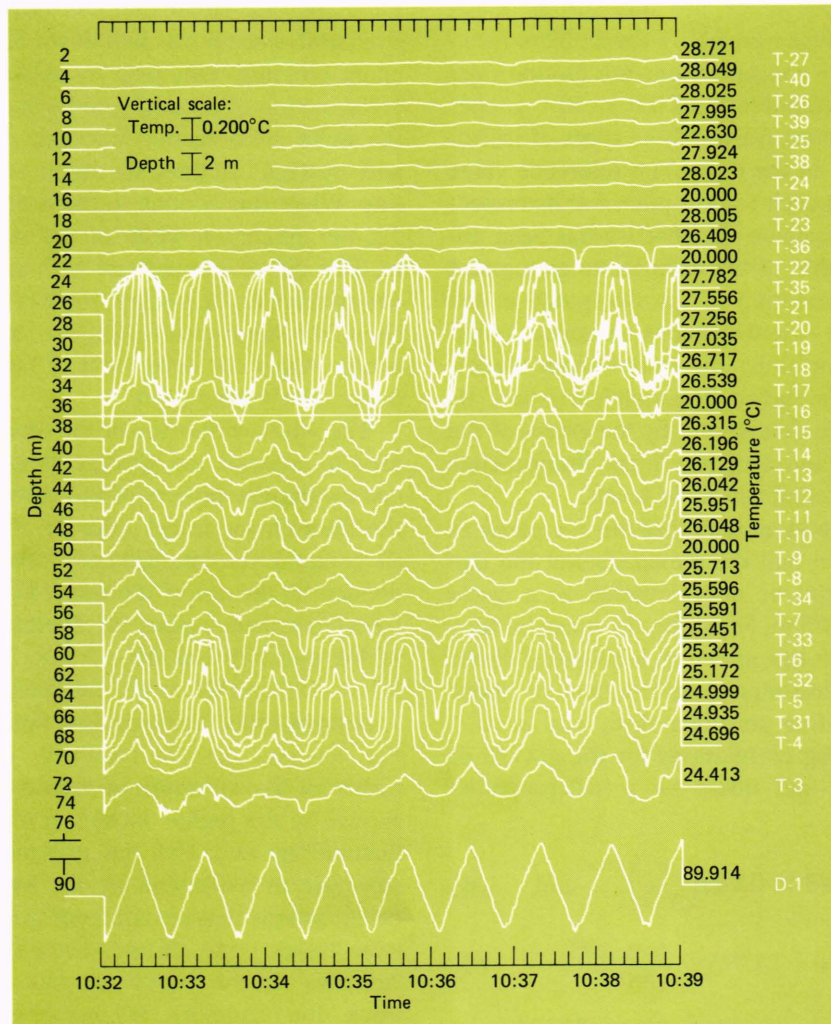


Fig. 12—Chain measurements from the yo-yo tow on August 8.

neath the mixed layer are two zones of high-temperature gradient separated by a zone of lesser gradient. Level portions of curves in these regions correspond to layers; nearly vertical features identify sheets.

These features are so lucidly identified that both the horizontal and vertical extent of the sheet-layer structure can be determined. However, some horizontal resolution is lost by the yo-yo method of towing as compared with the more conventional constant-depth tow. Therefore, the preferred type of tow to be used depends on the type of feature to be examined.

Figure 13 shows a 300-m profile taken on February 9, 1976, with the Plessey CTD. The temperature, salinity, and sigma T (σ_T , which equals $(\rho - 1)$ times 1000 g/cm³, where ρ is the density

of sea water) are plotted versus depth for the up and down casts of the instrument. The surface mixed layer extends to about 80 m, which is typical for that time of year and location. Just below the mixed layer is a region of temperature inversion that is also characteristic of the region in winter. A sharp increase in salinity takes place just below 70 m, reaching a maximum of 37.2‰ (parts dissolved salt per thousand parts solution) and then decreasing because of the subtropical underwater present in the area. Throughout the profiles, considerable fine structure is evident; some of it has a step-like appearance, and most features are consistent in both the down and up traces.

The data from Fig. 13 were used to obtain the B-V frequency N shown in Fig. 14. The profiles were generated from a running linear least-squares

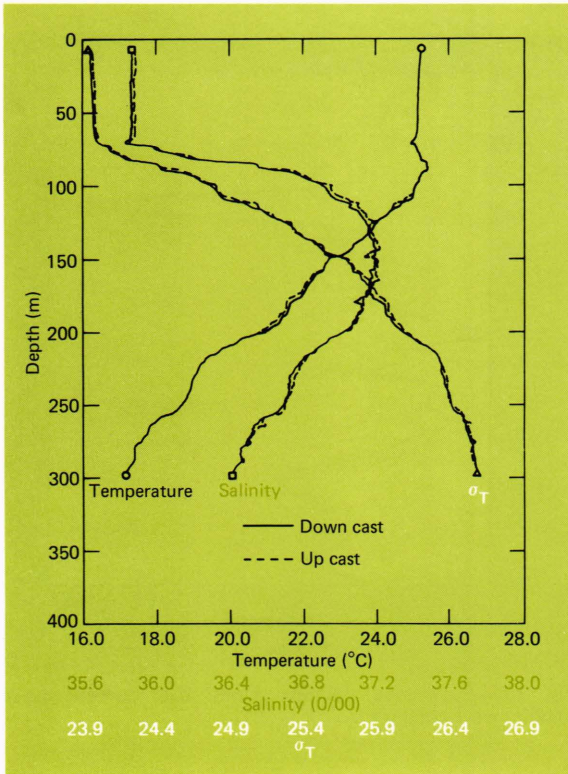


Fig. 13—Property measurements from a cast of the CTD on February 9.

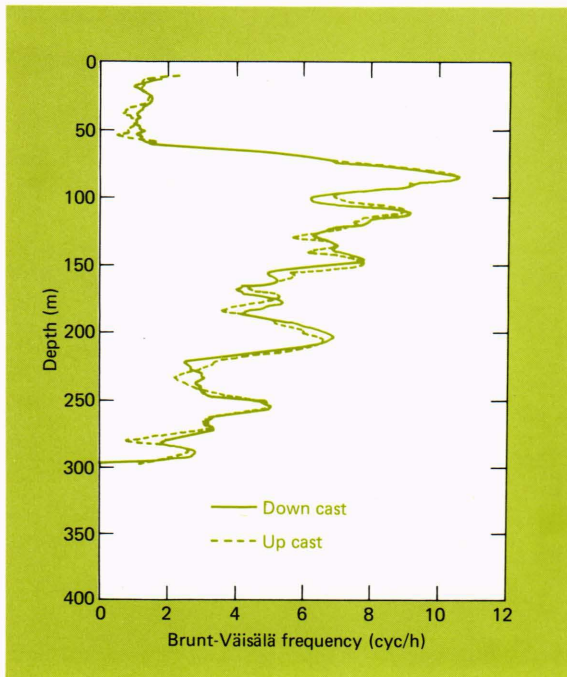


Fig. 14—Brunt-Väisälä frequency from the CTD cast on February 9.

fit to the density/pressure data, averaged over a depth interval of 15 m.⁵ The peak value of about 11 cyc/h reached just below the mixed layer is typical of the area during winter.

Figures 15 and 16 are constructed from data obtained with the Neil Brown CTD deployed from a surface ship to a mean depth of 40 m; they yo-yoed ± 5 m about that depth every 10 to 15 s between down and up legs while the ship was drifting. The depth interval and drop rate were established prior to the experiment so that within the Nyquist criterion (the frequency of the measurement cycle must be at least twice that of the maximum frequency to be resolved), wave motions with periods greater than 20 s could be discerned by using both down and up legs of the cast. The measurement technique was designed to allow short-period (<3-min) motions resulting from turbulent-like structure to be observed in the presence of longer-period (>5-min) motions caused by internal waves and of spatial variation caused by ship drift and currents.

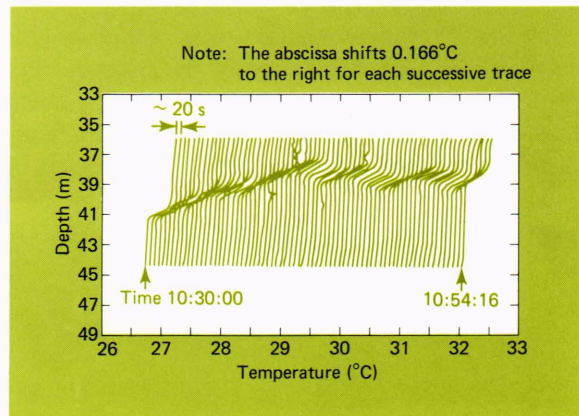


Fig. 15—"Waterfall" temperature display for yo-yo casts on August 21.

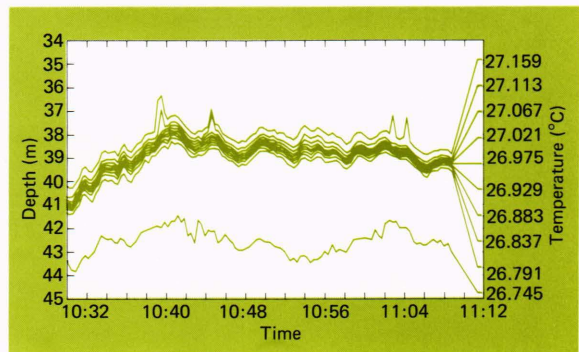


Fig. 16—Plot of isotherms from yo-yo casts of the CTD on August 21.

Figure 15 is a “waterfall” display of temperatures from a time series of down casts. Depth is the ordinate and temperature is the abscissa; the values given are for the first cast. For each successive cast, the temperature axis is translated a fixed amount to the right, 0.166°C in this case. In this way, qualitative features of the water structure are greatly enhanced, as is evident in Fig. 15. The sheet-layer structure (strong gradient—nearly constant temperature) and the oscillatory or wave-like perturbation in the depth of the sheet are clearly identified. Figure 16 is another way of displaying the data. It involves identifying particular values of one of the variables and plotting its depth dependence, as determined in each successive cast, versus time. Here, ten isotherms are shown spaced 0.046°C apart, between 26.745°C and 27.159°C . For simplicity, each value of an isotherm is plotted at the mean time of a particular cast. A minor change in the data-reduction scheme can be made to display data at actual rather than at mean time. The general oscillatory motion shown qualitatively in Fig. 15 is now depicted quantitatively.

Figure 17 shows the east-west component of current deduced from a drop of the shear-current profiler on February 9, 1976, at the point indicated in Fig. 8. The data are smoothed over 15-m increments. Agreed between the descent and ascent of

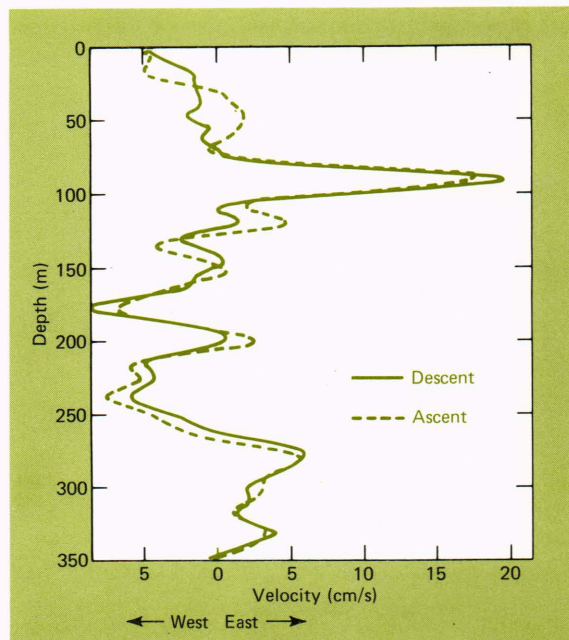


Fig. 17—East-west current from the current-shear profiler on February 9.

the profiler is good since major features are repeated. Current and shear levels just below the mixed layer are large and the structure throughout the profile is complex.

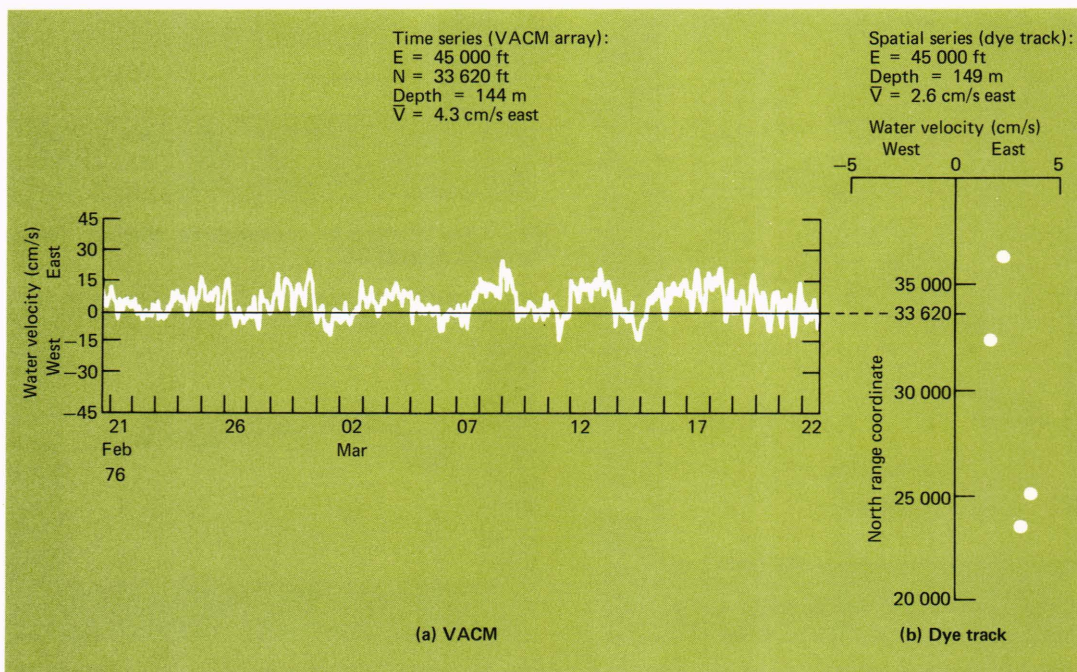


Fig. 18—East-west component of water velocity at St. Croix.

Currents as measured by a VACM on the mooring are compared with those deduced from the drifting of a dye track in Fig. 18. Figure 18a is a time series of one-hour averages of east-west currents at a depth of 144 m over a one-month period. The average current, \bar{V} , based on these data at this depth is 4.3 cm/s to the east. Figure 18b shows east-west currents deduced from chain tows made across a previously laid dye-track depth of 149 m. Although the data were taken a few weeks earlier, the interpolated value of 2 to 3 cm/s to the east at the same range coordinates is in general agreement with the VACM data. Moreover, the current measured with the shear profiler at a depth of 144 to 149 m is easterly at about 3 cm/s. This general consistency was observed even though the measurement location was about 3 km away.

By combining the east and north water velocities from the VACM, the total kinetic energy can be determined. The frequency distribution of the kinetic energy is shown in the smoothed power-spectral-density plot of Fig. 19. Peaks in the spectrum occur at the semidiurnal (~ 12 -h) and inertial (~ 39 -h) periods. Note also the falloff in the spectrum near the local B-V frequency, which is about 5 cyc/hr.

Concluding Remarks

The data presented herein are only a small sample of those obtained in the program. Improvements in many of the instrumentation systems have already been made, and techniques for deployment and recovery have been developed. To provide an open-ocean capability for those systems that depend on three-dimensional acoustical tracking (e.g., the current-shear profiler), a fully portable

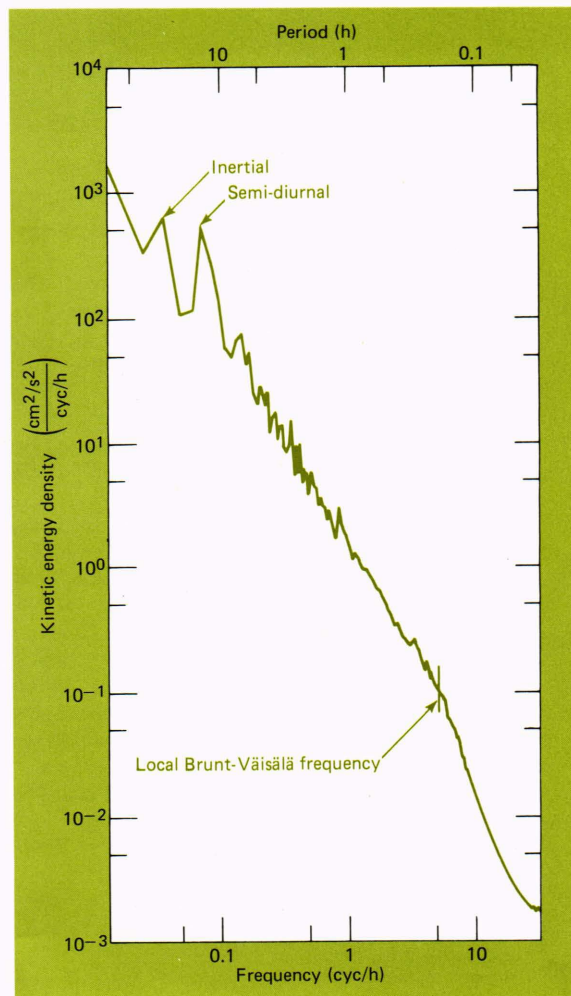


Fig. 19—Power spectral density at 144 m from February 20 to March 21.

acoustical-tracking range has been studied and determined to be feasible. APL's role in ocean research is well established; its fleet sails on.